Australian Journal of Basic and Applied Sciences, 9(27) August 2015, Pages: 487-496

ISSN:1991-8178

Australian Journal of Basic and Applied Sciences

Journal home page: www.ajbasweb.com

A Nonlocal Filtering with Coherence Vector based Weights for SAR Denoising

[1]D. Suresh and [2]Dr. P. Alli

[1] *Assistant Professor, PSNA College of Engg & Tech, Dindigul.*
[2] *Professor & Head, Velammal College of Engg & Tech, Madurai.*

ARTICLE INFO

Article history:
Received 23 June 2015
Accepted 25 August 2015
Available online 2 September 2015

Keywords: Synthetic-Aperture Radar, Non-Local (NL) means filter, Speckle Noise

ABSTRACT

Synthetic-Aperture Radar (SAR) imaging has become an efficient tool for the analysis about surfaces of Earth and other planets. However, the obtained images degraded from speckle noise, which affects the processes of SAR image interpretation, analysis and classification. One general solution is filtering, could improve the quality of the image by removing the noises and provide better estimation. Recently, a new category of image filters called Non-Local (NL) means filter has proved to be very successful in the removal of additive as well as multiplicative noises. NL filters works based on finding the self-similarity patches at various locations in the image and finds their average to replace the noisy pixels. Several extensions of NL filters has been proposed in the literature, still, the performance of NL filter could be improved by tuning its parameters like, window size, similarity measure, weight assignments and the number of iterations. In this paper, we have proposed a modified NL means filter with patches of coherence pixels for finding the self-similarity. The proposed filter seems to deal well with the statistical properties of speckle noise and the multi-dimensional nature of such data. Results are given on synthetic and SAR data to validate the proposed method. Numerical simulations demonstrate the success of this approach against several known despeckling methods.

© 2015 AENSI Publisher All rights reserved.

To Cite This Article: D. Suresh and Dr. P. Alli., A Nonlocal Filtering with Coherence Vector based Weights for SAR Denoising. ***Aust. J. Basic & Appl. Sci.,*** *9(27): 487-496, 2015*

INTRODUCTION

The current Synthetic Aperture Radar (SAR) imaging systems offers high-resolution images, however, suffer from strong speckle noises preventing the correctness of SAR image analysis. Even with the plenty of despeckling methods proposed in the literature, there is still a requirement for novel methods that can handle the SAR images efficiently to reduce speckle while preserving the spatial resolution as well as other imaging details like structures, edges and textures.

One simple method for despeckling is to find the average intensity of pixels in a rectangular window around each target pixel from different looks of a SAR image called spatial multilooking. However, the averaging also impairs the important signal features like edges, shapes, and textures. The point is that multilooking is just a basic nonadaptive form of parameter estimation: to remove speckle without degrading fine features, local image content must be taken into account.

The construction of efficient speckle reduction filter is a well-known problem since the advent of SAR imaging technology (Touzi, 2002). However, the success of SAR remote sensing accelerates the research activities for speckle reduction. Some of the most successful methods proposed in the literature for locally adaptive estimation are based on image models that enforce strong regularity constraints, either in the original domain (Denis *et al*., 2009), or in some transform domain (Achim *et al*., 2003). Recently, patch-based filtering has been proven as a most successful denoising in image analysis. The exploration of finding self-similar patches around the image space and denoising with their average, results in better preservation of edges, structures and textures.

Several improvements to multilooking have been proposed in the literature. The common underlying idea is to adapt the selection of samples used for covariance estimation in order to avoid mixing pixels belonging to different structures (e.g., blurring edges and strong scatterers by averaging them with their surrounding background). We suggest a classification of these methods into three main categories.

- A first category of approaches preserves the structural information by adaptively reintroducing the sub-region of the input image based on the

Corresponding Author: D. Suresh, Assistant Professor, PSNA College of Engg & Tech, Dindigul.
E-mail: sureshdgll@gmail.com

validity of the local stationary assumption, further improved by context adaptation. (Touzi, 2002).

- A second category of methods chooses the SAR images based local variations, since these methods are more sensitive, normally leads to complex optimization problems (Bhuiyan *et al*., 2007; Durand *et al*., 2010; Steidl and Teuber, 2010).
- The third category of approaches depends on adaptive selection of pixels, the same has been followed in this paper. The following text summarizes the methods proposed to perform adaptive selection:

Lee *et al*., (1999, 2003) proposed to locally select the best window based on the gradient of the amplitude image. Though this method produces good preservation of edges, the rapid change in window introduces more artifacts. Vasile *et al*., (2006) presented a region growing approach to find an adaptive neighbourhood pixels, as it eliminates the predefined window selection and size problem and outperforms the previous methods. But still, this method suffer from selection of bias for grouping the pixels, as because the speckle noise impairs the neighbours heavily. The approach for efficient pixel selection can be generalized by accounting the non-connected neighbourhoods has similar intensities. The basic idea was originated from Lee's sigma filter (Lee, 1983) and bilateral filter (Tomasi and Manduchi, 1998; D'Hondt *et al*., 2013). Further, the pixel selection is improved by finding the relative importance of them with the weighted comparison among its surrounded neighbours known as patches, this idea was coined by Buades *et al*., (2005) under the name Non-local (NL) means. After the success of NL filter, numerous extension have been proposed from this idea (Dabov *et al*., 2007; Katkovnik *et al*., 2010). Three different approaches have been followed in the literature to adapt nonlocal methods to SAR denoising(Deledalle *et al*., 2014):

a. The homomorphic approach, at first a logarithmic transform is applied to the image to convert the multiplicative noise as additive, then performs a standard nonlocal filter, and finally applied an exponential transform to map the filtered image back to their original dynamic range (Yang and Clausi, 2009; Makitalo *et al*., 2010).

b. The Bayesian approach interprets the NL-means as posterior means, where the posterior densities are calculated by comparing patches. A limitation here is the pre-filtering step, been resolved by sigma filter (Lee *et al*., 2009).

c. The statistical approach performs the pixel selection based on statistical test, once similar pixels are selected, the despeckling is performed by (weighted) maximum likelihood estimation (Deledalle *et al*., 2009, 2010, and 2011). Thus, contrary to the Bayesian approach, neither pre-estimation of a speckle-free image nor a sigma-range preselection is mandatory to drive the denoising procedure.

The patch-based nonlocal approach avoids the potentially dangerous identification between closeness and similarity and goes back to the original problem, trying to identify the pixels more similar to the target, irrespective (to a certain extent) of their spatial distance from it. However, the performance depends on appropriate selection of its parameters like window size, filter parameters and the number of iterations.

In this paper, we describe a generic framework, which is called Nonlocal Coherence Vector (NLCV) mean filter, for SAR denoising. Here, the classical nonlocal mean filter is applied with the weights assigned based on Coherence Vector (CV) of pixels from each window. The rest of the paper is organized as follows: Section 2 starts wtih the fundamental steps involved in nonlocal SAR despeckling and introduces the coherence vector calculation and explains the proposed NLCV filter. Section 3 discusses the experimental setup and the results are discussed in Section 4. Section 5 summarizes the conclusion of the paper.

2. Non-Local with Coherence Vector based Mean Filter:

2 *Non-Local Means Theory:*

At the core of the nonlocal approach stands the selection of suitable predictors based on their similarity with the target. The non-local means algorithm does not make the same assumptions about the image as other methods. Instead it assumes the image contains an extensive amount of self-similarity. Efros and Leung (1999) originally developed the concept of self-similarity for texture synthesis. An example of self-similarity is displayed in Figure 1 below. The figure shows three pixels *p*, *q1*, and *q2* and their respective neighbourhoods. The neighbourhoods of pixels *p* and *q1* are similar, but the neighbourhoods of pixels *p* and *q2* are not similar. Adjacent pixels tend to have similar neighbourhoods, but non-adjacent pixels will also have similar neighbourhoods when there is structure in the image (Buades *et al*., 2005). For example, in Figure 1 most of the pixels in the same column as *p* will have similar neighbourhoods to *p*'s neighbourhood. The self-similarity assumption can be exploited to denoise an image. Pixels with similar neighbourhoods can be used to determine the denoised value of a pixel.

Nonlocal estimation methods generally follow a three step process as shown in Figure 2. The first step identifies similar patches within an extended search window. Typical size for patch window is set from 3x3 to 11x11 and the search window size is set from 21x21 to 39x39. Once the patches have been chosen within the search window, they are assigned with relative weights. Either based on the canter pixel, the central patch, or all selected pixels, the patches are combined in the second step. In the last step, the

similar patches are averaged to produce the denoised image.

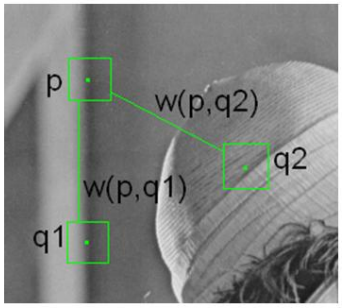

Fig. 1: Example of self-similarity in an image. Pixels *p* and *q1* have similar neighbourhoods, but pixels *p* and *q2* do not have similar neighbourhoods. Because of this, pixel *q1* will have a stronger influence on the denoised value of *p* than *q2*.

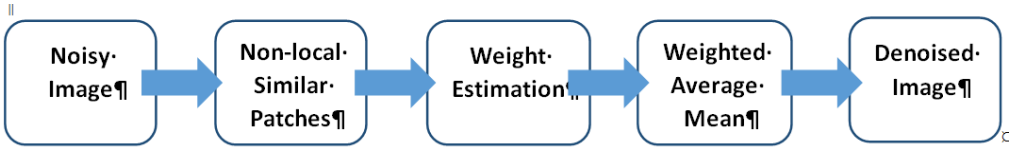

Fig. 2: Nonlocal estimation in action: processing at pixel x (ref).

Consider the area of an image (Ω), and p and q are two pixels within the image, then the NL means filter is (Buades *et al*., 2011):

$$u(p) = \frac{1}{N(p)} \int_{\Omega} v(q)\, w(p,q)\, dq$$

Where u(p) is the denoised value of the image at pixel p, v(q) is the noisy intensity value of the image at point q. w(p, q) is the weighting function, and the integral is evaluated over $\forall q \in \Omega$. N(p) is the normalizing factor, given by:

$$N(p) = \int_{\Omega} w(p,q)\, dq$$

For an image with discrete pixels, the NL means filter is implemented with the following equation.

$$u(p) = \frac{1}{N(p)} \sum_{q \in S(p,t)} v(q)\, w(p,q), N(p) = \sum_{q \in S(p,t)} w(p,q)$$

Where S(p, t) indicates a search window of size 2t+1 × 2t+1 pixels centered at p.

Step 1: Defining patch Similarities:

The first step of NL means filter is to find the similar patches within the search window through a (dis)similar measure. The similarity between two patches is generally defined by sum of the similarity of each pair of corresponding pixels in the two noisy patches. The following are the possible approaches to derive the pixel-wise similarity.

- Detection Approach - It is formulated as a hypothesis test, where the null hypothesis corresponds to no difference and the alternative one to a difference (Deledalle, 2012).
- Information Approach - here also the detection approach is used, but the hypothesis test is performed with pre-estimates of the parameters (Torres *et al*., 2014).
- Geometric Approach - This approach uses a metric like geodesic and Riemannian distances, which is more suitable to SAR data (D'Hondt *et al*., 2013).
- Estimation Approach - The SAR data dependent metric may suffer from a systematic bias, so, a weighted average estimation based on exponential kernel is used in this approach, and becomes successful irrespective of the modality, the noise statistic, of the patch size (Lee *et al*., 2009). This approach is followed in this paper.

Each pixel is a weighted average of all the pixels in the image. The weights are based on the similarity between the neighbourhoods of pixels *p* and *q*. For example, in Figure1 above the weight *w(p,q1)* is much greater than *w(p,q2)* because pixels *p* and *q1* have similar neighbourhoods and pixels *p* and *q2* do not have similar neighbourhoods. In order to compute the similarity, a neighbourhood must be defined. Here the squared Euclidean distance (d^2) defines the neigbourhood between pixels p and q, which is defined as d^2 (S(p, f), S(q, f)) of the size 2f+1 × 2f+1 patch windows centered respectively at pixels p and q.

$$d^2(S(p,f), S(q,f)) = \frac{1}{(2f+1)^2} \sum_{j \in S(0,f)} (v(p+j) - (v(q+j))^2$$

That is, each pixel value is restored as an average of the most similar pixels. So far, each pixel value is the result of the average of the similar pixels, further an exponential kernel is used in order to comput the weights

$$w(p,q) = e^{-\frac{\max(d^2-2\sigma^2,0.0)}{h^2}}$$

whereσ denotes the standard deviation of the noise and h is the filtering parameter set depending on the value of σ. The weight function is set in order to average similar patches up to noise. That is, patches with square distance smaller than $2\sigma^2$ are set to 1, while larger distances decrease rapidly accordingly to the exponential kernel.

Step 2: Estimation of Radar properties:

After the selection of a stack of patches and/or computation of relative weights during the first step of the nonlocal estimation method, these patches are combined in a second step to form an estimate of the radar properties. This combination can be a simple (weighted) averaging as in the NL-means, or a more evolved estimator.The most common estimators for patch-based denoising of SAR images are:

SME/WMSE: This is the very common estimator followed in most of the NL means filtering algorithms, the Weighted Sample Mean Estimator (WSME) is defined as

$$WMSE(p) = \frac{\sum_q w(p,q)N(q)}{\sum_q w(p,q)}$$

The WSME is not a good estimator in case of amplitude, and it is not noise distribution specific. Deledalle *et al*., (2009) proposed Weighted Maximum Likelihood Estimator (WMLE) defined as

$$WMLE(p) = \max_u \sum_q w(p,q)\log p[v(q)|u]$$

But, WMLE is suitable only for InSAR images with particular structures. Kervrann *et al*., (2007) proposed Bayesian NL-means that make use of linear combination of pre-estimated patches, and results in coarse estimation and requires a smoothing parameter to avoid weighting too much patches. In this paper, we have used WSME for the estimation.

The weight of the reference pixel p in the average is set to the maximum of the weights in the neighbourhood S(p, t). This setting avoids the excessive weighting of the reference point in the average. Otherwise, w(p,q) should be equal to 1 and a larger value of h would be necessary to ensure the noise reduction. By applying the above averaging procedure we recover a denoised value at each pixel p.

2.1 Intensity Coherence Vector:

Intuitively, the pixel's intensity coherence is defined as the degree to which pixels of that intensity are members of large similarly-colored regions. These significant regions are referred as coherent regions, and it is observed that they are important in characterizing images. The coherence measure ICV classifies pixels as either coherent or incoherent. Coherent pixels are a part of some sizable contiguous region, while incoherent pixels are not. Anintensity coherence vector represents this classification for each pixel in the image based on their similarity of intensity values with its neighbours. ICV's prevent coherent pixels in one image from matching incoherent pixels in another. This allows fine distinctions that cannot be made with histograms. This property of ICV is used here to identify the non-local pixels at every sub-region received from improved watershed segmentation algorithm. The following text explains the computation of ICV measure.

Computing ICV's:

The first step in computing ICV is similar to the computation of a histogram. Initially the image is discretized into 'nc' number of distinct intensities to eliminate the small oscillations between neighboring pixels. The next step is to classify the pixels within a given region as either coherent or incoherent. A coherent pixel is a part of a large group of pixels of the same color, while an incoherent pixel is not. The pixel group is determined by computing connected components. A connected component C is a maximum set of pixels in such a way that for any two pixels p, p' ∈ C, there is a path in C between p and p'. (Formally, a path in C is a sequence of pixels p = p_1, p_2, ... ,p_n = p' such that each pixel p_i is in C and any two sequential pixels p_i, p_{i+1} are adjacent to each other. Two pixels are considered to be adjacent if one pixel is among the eight closest neighbours of the other.In other words, diagonal neighbors are included.) Note that connected components are computed within a given discretized intensity bucket. This effectively segments the sub-region based on the discretized space.

Connected components can be computed in a linear time. When this is complete, each pixel will belong to exactly one connected component. Then the pixels are classified as either coherent or incoherent depending on the size in pixels of its connected component. A pixel is coherent if the size of its connected component exceeds a fixed value 'k'; Otherwise, the pixel is incoherent. For a given discretized intensity range, some of the pixels with that intensity will be coherent and some will be incoherent. Let us call the number of coherent pixels of the j^{th} discretized color α_j and the number of incoherent pixels β_j. Clearly, the total number of pixels with that color is $\alpha_j + \beta_j$.

For each discrete pixel value, the pair (α_j,β_j) is computed and it is named as the coherence pair for the intensity. The intensity coherence vector for the image consists of

$<(\alpha_1,\beta_1), \ldots, (\alpha_n, \beta_n)>$

This is a vector of coherence pairs, one for each discretized intensity value. A numerical example for computing ICVs can be referred in Pass *et al*., (1997).

2.2 The Proposed NL-CV Filter:

With the conceptual backgrounds of NL means filter and intensity coherence vector, a novel filter is proposed in this paper. Here, the non-local patch weights are calculated with the coherence pixels rather than considering the entire pixels in the patch window.

The proposed work has been implemented in two steps. Initially the image is computed with ICV, and the pixels are labelled according to their coherence. Hence the pixels with the similar intensities are grouped together and assigned with unique labels. The labels are then maintained in a separate matrix of size M×M same as original image size. For an example, Figure 3(a), shows sample image of size 10×10, after ICV, the corresponding pixel locations are labelled according to their coherence (Figure 3(b) and 3(c)). The coherence pixels are shaded with different colors as shown in Figure 3(b), and the same is labelled in Figure 3(c).

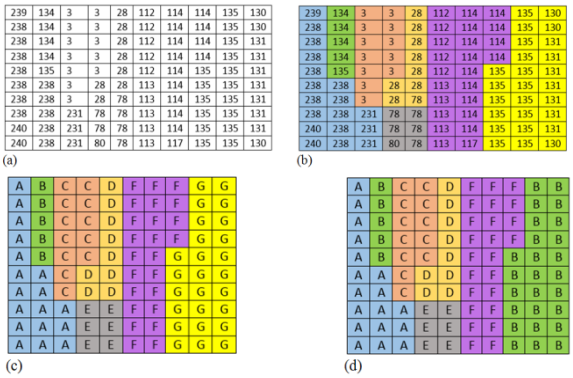

Fig. 3: Computing ICV. (a) Sample image pixel intensities, (b) Coherent Regions, (c) Coherent discrete Labels for each region, (d) Unique labels for each intensity coherence.

It should be noted that, though the intensity of the labels B & G and same in range, the labels are different as they are not belongs to the same region. So, the image is further traced for each intensity to change the labels of same intensity range into one, as shown in the Figure 3(d).

In the second step the NL means filter is applied based on coherence labels received from the previous step.For an image, at every pixel p, the search patch window is extracted, and trace for the similar patches within the search window to find the non-local weighted average mean. The similarity is found based on Euclidian distance, in case of typical NL means filter, the distance measure is calculated with each corresponding pixels between two patches, But in the proposed method, the distance measure is calculated only if the corresponding pixels are belongs to the same coherence label, otherwise, those pixels are ignored from distance calculation. Figure 4 illustrates the proposed approach, the figure 4(a) shows the two patches to be compared, centered at (2,9) and (9,9), the distance is calculated only with the pixels from the second and third column of each patches, while the first column of pixels are ignored as they are not coherently same.

Iterative Weight Updation:

The calculated weights between the patches are iteratively refined for better weight estimation. The weight comprises of similarity between the noisy patches and the similarity between the restored patches. Once the patches are denoised, the algorithm is executed again with the denoised patches to refine the weights iteratively. Let us consider the weight w_i estimated at i^{th} iteration, the patch similarity can be extended by using the knowledge of weight w_{i-1} from the previous iteration.

The following algorithm illustrates the proposed NL-CV means filter:

1. Read the input image
2. Estimate Intensity Coherence Vector
   a. Initially the coherence label is identified for each pixel of the image.
   b. A label matrix is created with coherence label.
   c. The labels are traced to make unique label for the pixels with same intensity values.
3. Apply Non-Local Means Filter
   a. For each pixel
      i. Extract a patch centered at p
      ii. Trace the search window, locate another patch centered at q
      iii. Find the similarity with Euclidian distance based on coherence labels
      iv. Find the weights
      v. Update the pixels with WSME/WMLE estimation
   b. Repeat step-a, until the change between two consecutive estimates is negotiable.
4. Output the denoised image.

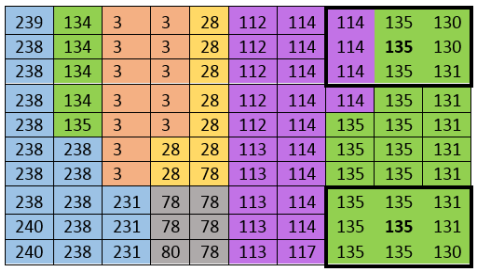

(a)

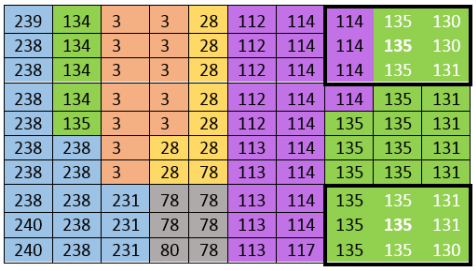

(b)

Fig. 4: Coherence Vector based NL-mean Calculation. (a) Patches under similarity comparison, (b) Pixels to be considered for distance calculation.

3. Experimental setup:

This section presents the parameter setting for the proposed NL-CV filter. The non-local means algorithm has three parameters. The first parameter, *h*, is the weight-decay control parameter which controls where the weights lay on the decaying exponential curve. If *h* is set too low, not enough noise will be removed. If *h* is set too high, the image will become blurry. When an image contains white noise with a standard deviation of σ,*h* should be set between 10σ and 15σ.

The second parameter*f* is the radius of the neighbourhoods used to find the similarity between two pixels. If *f* is too large, no similar neighbourhoods will be found, but if it is too small, too many similar neighbourhoods will be found. Common values for *f* are 3 and 4 to give neighbourhoods of size 7x7 and 9x9, respectively.

The third parameter, *t*, is the radius of a search window. Because of the inefficiency of taking the weighted average of every pixel for every pixel, it will be reduced to a weighted average of all pixels in a window. The window is centered at the current pixel being computed. Common values for *t* are 7 and 9 to give windows of size 15x15 and 19x19, respectively. With this change the algorithm will take a weighted average of 15^2 pixels rather than a weighted average of M^2 pixels for MxM size image.

RESULTS AND DISCUSSION

In this paper, both simulated and real SAR images are used to analyze the performance of the proposed SAR denoising method. Initially, the image is multiplied with speckle noise to degrade them. Thus, the original images are treated as the true values and are used as numerical measures to assess the performance. In this experiment, seven other existing NL means methods are selected to compare with the proposed method. The selection of these methods is based on both availability of the codes and their relevance to this work.

4.1 Synthetic Images Database:

A variety of image sources are considered in this experiment, including the benchmark test image, Lena. A synthetically speckled image is generated by a noise-free image with speckle noise. L-look amplitude speckled Lena image of size 512×512 disturbed by fully developed speckle is taken for experiments. The proposed algorithm was implemented in MatLab® environment, the Lena image is one of the test image freely available within the MatLab environment itself.

4.2 Sar Images Database:

To validate the effectiveness of proposed algorithm, the SAR images from NASA repository has been used (http://webmap.ornl.gov/ogcdown/dataset.jsp?ds_id= 993). This data set provides Synthetic Aperture Radar (SAR) images for 42 selected sites from various monitoring networks including Fluxnet, Ameriflux, LTER, and the Greenland Climate Network (GC-Net).There is at least one image for all 42 sites and six sites have multiple images. The scenes are in GeoTIFF format in Universal Transverse Mercator (UTM) projection and 15 meter resolution. The SAR images are subset scenes of approximately 60 km x 70 km that include an established site in one of the monitoring networks. These scenes are distributed as 3 band geotif files with appropriate projection information defined within the file. The acquisition mode for all data is Fine Beam Double Polarization or FBD with the

HH/HV polarization. The HH and HV channels are distributed as 3 channels to allow for an intuitive image display. The HH band is displayed in red and blue channels and HV band is displayed in green channel. The source of the data is the PALSAR (Phased Array type L-band Synthetic Aperture Radar) sensor flying on the Advanced Land Observing Satellite (ALOS). The PALSAR data are in dual Polarization, HH+HV, mode. Bands HH (red and green) and Band-HV (blue) can be used to visualize land use patterns. The resulting images show vegetation in shades of green and barren land in shades of pink or purple. The backscattering coefficient or Normalized Radar Cross Section (NRCS) are also provided as gray scale images.

4.3 Performance Evaluation:

The performance of the proposed algorithm is evaluated with three different measures: Peak-Signal to Noise Ratio (PSNR), Equivalent Number of Looks (ENL), and the Edge Preservation Degree based on Ratio of Average (EPD-ROA).

Peak Signal to Noise Ratio (PSNR) provides the quality of the image in terms of the power of the speckled image and despeckled image. Mean Square Error (MSE) quantifies the amount of despekling between the noisy (original) and denoised images.

$$PSNR = 10\ \log_{10}\frac{255^2}{MSE}\ ,MSE = \frac{1}{M^2}\sum_{i=1}^{M}\sum_{j=1}^{M}(x_{ij}-y_{ij})^2$$

Edge-Preservation Degree Based on Ratio Average (EPD-ROA) (Feng *et al*., 2011) is an effective tool to evaluate the edge preservation for real SAR image, which is stable for different types of edge images and is only affected by the speckle level. The ideal value of EPD-ROA is equal to one. The EPD-ROA is closer to one, which means better ability of edge preservation.

Equivaluent Number of Looks (ENL) (Parrilli *et al*., 2012) measures the degree of speckly reduction in a homogeneous region. The value of ENL also depends on the size of the tested region. Theoretically it should be large enough to provide a robust estimation of the value of ENL and to meet the homogeneous hypothesis in that region, and a higher ENL value corresponds to better speckle suppression. A large ENL value represents better quality performance of denoised image.

ENL = μ^2 / σ^2

$$\mu = \frac{1}{M^2}\sum_{i=1}^{M}\sum_{j=1}^{M}x_{ij},\ \sigma = \frac{1}{M^2}\sum_{i=1}^{M}\sum_{j=1}^{M}(x_{ij}-\mu)^2$$

Where μ is the mean value of the original image, and σ is the standard deviation of the noise, which finds the amount of speckle noise added in the image. The lower σ represents the clear image.

Besides the visual quality, the equivalent number of looks (ENL), the edge preservation degree based on ratio of average (EPD-ROA) also used to verify the denoising quality. The EPD-ROA is a novel measurement method of edge preservation degree based on ratio of image, and the EPD-ROA can be expressed as:

$$EPD-ROA = \frac{\sum_{i=1}^{m}|I_{D1}(i)/I_{D2}(i)|}{\sum_{i=1}^{m}|I_{O1}(i)/I_{O2}(i)|}$$

where m is the pixel number of the selected area, I_{D1} and I_{D2} represent the adjacent pixel values of the despeckling image along a certain direction. Similarly, I_{O1} and I_{O2} represent the adjacent pixel values of the speckled image.

The performance of the proposed NL-CV filter is compared with the seven other existing non-local means filtering methods:Probabilistic Patch-Based (PPB) weights(Deledalle *et al*., 2009), Pretest-NLM (Chen *et al*., 2011), Bayesian NLM(Zhong *et al*., 2011), BM3D (Parrilli *et al*., 2012), Bilateral NLM(D'Hondt *et al*., 2013), Stochastic NLM (Torres *et al*., 2014) and NL-SAR (Deledalle *et al*., 2015), with four different σ values (10, 20, 40 and 60) and four different looks (L = {1, 2, 4, 16}).

Table 1: PSNR values of estimated images using different denoising methods.

METHODS	Lena Image							
	σ = 10	σ = 20	σ = 40	σ = 60	L = 1	L = 2	L = 4	L = 16
NL – CV	29.59	28.36	29.33	27.18	28.15	24.58	25.64	23.40
BM3D	27.22	27.47	26.74	26.37	25.69	21.72	20.32	20.11
Pretest-NLM	16.90	17.36	26.88	26.15	16.46	20.48	19.14	23.78
Bayesian NLM	22.70	22.56	21.39	20.88	22.35	20.93	19.20	18.36
Bilateral NLM	24.49	23.36	24.84	24.83	25.42	24.80	20.83	20.27
Stochastic NLM	16.46	22.28	15.54	17.57	19.76	22.35	17.44	18.83
PPB	19.18	17.00	17.74	15.59	19.25	11.68	16.78	12.59
NL – SAR	23.20	17.13	22.01	15.48	15.52	14.69	12.48	12.49
	SAR Image							
NL – CV	29.62	28.88	29.14	26.54	28.80	25.14	27.56	22.95
BM3D	28.68	26.28	25.54	25.43	25.90	22.60	20.80	18.77
Pretest-NLM	17.59	17.31	25.94	24.46	17.68	21.53	17.79	15.47
Bayesian NLM	21.53	21.71	22.78	20.06	20.79	20.02	18.62	17.67
Bilateral NLM	24.27	23.99	26.24	26.47	24.57	23.05	19.49	18.71
Stochastic NLM	18.27	21.96	14.26	16.13	19.94	21.31	16.05	20.18
PPB	17.42	16.64	17.81	17.53	18.72	13.57	16.64	12.58
NL – SAR	24.84	16.28	21.87	16.54	15.21	13.41	12.99	13.69

Table 1 provides the performance analysis of the proposed method on PSNR measure for both synthetic and real SAR image data, from the quantification it is noted that the proposed NL-CV

filter is able to outperform the other methods with higher PSNR values. The increase in noise standard deviation (σ) and number of looks (L) reduces the performance of the despeckling. Next to the proposed method the BM3D and NL-SAR methods achieves better despeckling. In terms of consistency, the proposed NL-CV and the BM3D has steady performance than the others.

Table 2 provides the performance analysis of the proposed method on ENL measure. Once again the proposed method achieves the higher ENL value than the others, whereas the NL-SAR method performance is decreased for this measure. The BM3D results are closer to the performance of the proposed method and next the Pretest-NLM method has the better performance in the row. In overall, based on ENL, the denoising methods including the proposed method are not consistent, this could be because of the random noise distribution and the higher number of looks.

Edge preservation in denoising is an effective parameter to quantify the performance. Table 3 provides the performance analysis of the proposed method on EPD-ROA measure. Here also the proposed method outperforms with the other methods. The proposed filter makes use of the coherence label and the labels identifies the edges with the unique label that is the reason for the higher EPD-ROA.

Table 2: ENL values of estimated images using different denoising methods.

METHODS	Lena Image							
	σ = 10	σ = 20	σ = 40	σ = 60	L = 1	L = 2	L = 4	L = 16
NL – CV	81.82	76.07	81.37	83.53	47.66	57.42	52.17	43.00
BM3D	76.95	23.26	67.31	47.59	40.20	50.15	33.50	37.14
Pretest-NLM	46.04	44.69	48.89	10.69	28.34	38.79	10.86	11.33
Bayesian NLM	15.40	31.25	46.23	24.72	30.28	54.06	36.94	33.12
Bilateral NLM	16.20	19.74	73.79	44.81	17.16	56.69	45.38	36.30
Stochastic NLM	24.31	23.83	26.44	63.44	34.57	31.11	39.71	30.15
PPB	28.05	11.20	11.79	15.05	5.89	9.05	16.43	5.35
NL – SAR	24.07	40.50	61.53	14.74	44.64	11.29	38.20	34.98
	SAR Image							
NL – CV	84.61	80.55	82.76	76.82	55.21	50.38	56.47	40.84
BM3D	82.17	19.60	60.35	40.18	42.63	45.73	24.62	35.04
Pretest-NLM	36.10	37.05	49.83	15.89	32.76	38.99	14.77	20.82
Bayesian NLM	13.21	24.97	40.98	28.20	23.40	37.37	34.63	29.84
Bilateral NLM	15.14	27.46	79.09	46.31	20.75	42.45	49.35	23.01
Stochastic NLM	23.21	14.50	17.83	57.58	27.21	33.81	47.80	34.54
PPB	28.69	1.47	16.64	17.67	1.94	7.08	8.88	13.69
NL – SAR	20.02	38.58	57.60	15.18	51.47	19.51	34.43	42.67

Table 3: EPD-ROA values of estimated images using different denoising methods.

METHODS	Lena Image							
	σ = 10	σ = 20	σ = 40	σ = 60	L = 1	L = 2	L = 4	L = 16
NL – CV	0.9299	0.9346	0.7009	0.9514	0.8901	0.7876	0.8246	0.8434
BM3D	0.9000	0.7899	0.5380	0.7724	0.6949	0.5299	0.7659	0.5918
Pretest-NLM	0.7157	0.7749	0.6200	0.7454	0.6208	0.6174	0.8239	0.6842
Bayesian NLM	0.7553	0.5725	0.5617	0.7446	0.7020	0.6766	0.7255	0.8128
Bilateral NLM	0.5909	0.7265	0.5920	0.6689	0.5482	0.6106	0.7735	0.6901
Stochastic NLM	0.6319	0.8110	0.6200	0.9500	0.5660	0.5077	0.6482	0.5406
PPB	0.5728	0.6755	0.7086	0.6846	0.4710	0.5215	0.4723	0.4647
NL – SAR	0.5680	0.7566	0.5248	0.5556	0.6781	0.5845	0.5945	0.7879
	SAR Image							
NL – CV	0.9210	0.8846	0.6829	0.9748	0.9051	0.7883	0.8412	0.8479
BM3D	0.8331	0.8043	0.5408	0.8180	0.7016	0.5748	0.7808	0.5878
Pretest-NLM	0.7322	0.7956	0.5939	0.7506	0.6314	0.6272	0.8270	0.6453
Bayesian NLM	0.8002	0.5957	0.5449	0.7819	0.7467	0.6813	0.7404	0.8581
Bilateral NLM	0.5968	0.6883	0.5832	0.7057	0.5446	0.6260	0.7758	0.6634
Stochastic NLM	0.6813	0.8519	0.6096	0.9781	0.5781	0.4849	0.6735	0.5461
PPB	0.5458	0.6705	0.6633	0.6938	0.4683	0.5266	0.5104	0.4234
NL – SAR	0.5327	0.7477	0.5586	0.5257	0.6560	0.5347	0.6261	0.8048

Figure 5 and 6 illustrates the output of the proposed NL-CV filter for synthetic and real SAR images (where the noise standard deviation is set to 40 and the number of looks is 4).

4. Conclusions:

This paper proposed a modified Non-Local (NL) means filter for SAR image denoising. For an image, similar patches are identified and their weighted mean values are estimated to denoise the pixels centered in the patch. The patches are rectangular window in general, and all the pixels in the window are considered for finding the similarity. Here in the proposed method, for each pixel, the intensity Coherence Vector (CV) is identified and labelled the same. At the time of similarity measure, the pixels in

the patches centered at p, whichever has the same coherence label alone consider. The weight estimation procedure is repeated for certain number of times to refine the weights. The performance of the proposed method is analyzed with PSNR, ENL and EPD-ROA methods, and compared with seven other existing NL mean filter denoising. The results indicate that the NL-CV filter outperforms the other methods with higher quantitative measures.

Fig. 5: Synthetic Image Denoising. (a) Noisy Image, (b) PPB, (c) NL – SAR, (d) Bilateral NLM, (e) Bayesian NLM, (f) Pretest NLM, (g) BM3D, (h) NL – CV.

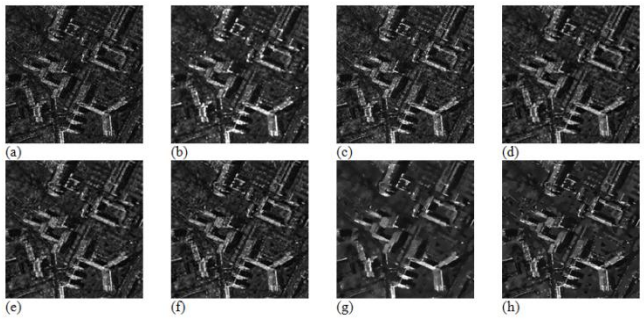

Fig. 6: Real SAR Image Denoising. (a) Noisy Image, (b) PPB, (c) NL – SAR, (d) Bilateral NLM, (e) Bayesian NLM, (f) Pretest NLM, (g) BM3D, (h) NL – CV.

REFERENCES

Achim, A., P. Tsakalides, A. Bezerianos, 2003. SAR image denoising via Bayesian wavelet shrinkage based on heavy-tailed modeling. IEEE Transactions on Geoscience and Remote Sensing, 41(8): 1773-1784.

Bhuiyan, M.I.H., M.O. Ahmad, M.N.S. Swamy, 2007. Spatially adaptive wavelet-based method using the Cauchy prior for denoising the SAR images. IEEE Transactions on Circuits and Systems for Video Technology, 17(4): 500-507.

Buades, A., B. Coll, J.M. Morel, 2005. A review of image denoising algorithms, with a new one. Multiscale Modeling& Simulation, 4(2): 490-530.

Buades, A., B. Coll, J.M. Morel, 2011. Non-local means denoising. Image Processing On Line,.

Chen, J., Y. Chen, W. An, Y. Cui, J. Yang, 2011. Nonlocal filtering for polarimetric SAR data: A pretest approach. IEEE Transactions onGeoscience and Remote Sensing, 49(5): 1744-1754.

Dabov, K., A. Foi, V. Katkovnik, K. Egiazarian, 2007. Image denoising by sparse 3-D transform-domain collaborative filtering. IEEE Transactions onImage Processing, 16(8): 2080-2095.

Deledalle, C.A., L. Denis, F. Tupin, 2009. Iterative weighted maximum likelihood denoising with probabilistic patch-based weights. IEEE Transactions onImage Processing, 18(12): 2661-2672.

Deledalle, C.A., L. Denis, F. Tupin, 2011. NL-InSAR: Nonlocal interferogram estimation. IEEE Transactions on Geoscience and Remote Sensing, 49(4): 1441-1452.

Deledalle, C.A., L. Denis, F. Tupin, 2012. How to compare noisy patches? Patch similarity beyond.

Deledalle, C.A., L. Denis, G. Poggi, F. Tupin, L. Verdoliva, 2014. Exploiting patch similarity for SAR image processing: the nonlocal paradigm. Signal Processing Magazine, IEEE, 31(4), 69-78.

Deledalle, C.A., L. Denis, F. Tupin, A. Reigber, M. Jäger, 2015. NL-SAR: A unified nonlocal framework for resolution-preserving (Pol)(In) SAR denoising. IEEE Transactions onGeoscience and Remote Sensing, 53(4): 2021-2038.

Deledalle, C. A., F. Tupin, L. Denis, 2010. Polarimetric SAR estimation based on non-local means. 2010 IEEE International Geoscience and Remote Sensing Symposium (IGARSS), (pp: 2515-2518).

Denis, L., F.E. Tupin, J. Darbon, M. Sigelle, 2009. Joint regularization of phase and amplitude of InSAR data: Application to 3-D reconstruction. IEEE Transactions on Geoscience and Remote Sensing, 47(11): 3774-3785.

D'Hondt, O., S. Guillaso, O. Hellwich, 2013. Iterative bilateral filtering of polarimetric SAR data. IEEE Journal ofSelected Topics in Applied Earth Observations and Remote Sensing, 6(3): 1628-1639.

Durand, S., J. Fadili, M. Nikolova, 2010. Multiplicative noise removal using L1 fidelity on frame coefficients. Journal of Mathematical Imaging and Vision, 36(3): 201-226.

Efros, A., T.K. Leung, 1999. Texture synthesis by non-parametric sampling. In Proceedings of the Seventh IEEE International Conference on Computer Vision, 2: 1033-1038). IEEE.

Feng, H., B. Hou, M. Gong, 2011. SAR image despeckling based on local homogeneous-region segmentation by using pixel-relativity measurement. IEEE Transactions onGeoscience and Remote Sensing, 49(7): 2724-2737.

Gaussian noise, International journal of computer vision, 99(1): 86-102.

Katkovnik, V., A. Foi, K. Egiazarian, J. Astola, 2010. From local kernel to nonlocal multiple-model image denoising. International journal of computer vision, 86(1): 1-32.

Kervrann, C., J. Boulanger, P. Coupé, 2007. Bayesian non-local means filter, image redundancy and adaptive dictionaries for noise removal. In Scale Space and Variational Methods in Computer Vision (pp: 520-532). Springer Berlin Heidelberg.

Lee, J.S., 1983. Digital image smoothing and the sigma filter. Computer Vision, Graphics, and Image Processing, 24(2): 255-269.

Lee, J.S., S.R. Cloude, K.P. Papathanassiou, M.R. Grunes, I.H. Woodhouse, 2003. Speckle filtering and coherence estimation of polarimetric SAR interferometry data for forest applications. IEEE Transactions on Geoscience and Remote Sensing, 41(10): 2254-2263.

Lee, J.S. M.R. Grunes, G. De Grandi, 1999. Polarimetric SAR speckle filtering and its implication for classification. IEEE Transactions on Geoscience and Remote Sensing, 37(5): 2363-2373.

Lee, J.S., J.H. Wen, T.L. Ainsworth, K.S. Chen, A.J. Chen, 2009. Improved sigma filter for speckle filtering of SAR imagery. IEEE Transactions onGeoscience and Remote Sensing, 47(1): 202-213.

Makitalo, M., A. Foi, D. Fevralev, V. Lukin, 2010. Denoising of single-look SAR images based on variance stabilization and nonlocal filters. International Conference on Mathematical Methods in Electromagnetic Theory (MMET), (pp: 1-4).

Parrilli, S., M. Poderico, C.V. Angelino, L. Verdoliva, 2012. A nonlocal SAR image denoising algorithm based on LLMMSE wavelet shrinkage. IEEE Transactions onGeoscience and Remote Sensing, 50(2): 606-616.

Pass, G., R. Zabih, J. Miller, 1997. Comparing images using color coherence vectors, In Proceedings of the fourth ACM international conference on Multimedia, 65-73.

Steidl, G., T. Teuber, 2010. Removing multiplicative noise by Douglas-Rachford splitting methods. Journal of Mathematical Imaging and Vision, 36(2): 168-184.

Tomasi, C., R. Manduchi, 1998. Bilateral filtering for gray and color images. Sixth International Conference on ComputerVision, 1998. (pp: 839-846). IEEE.

Torres, L., S.J. Sant'Anna, C. da Costa Freitas, A.C. Frery, 2014. Speckle reduction in polarimetric SAR imagery with stochastic distances and nonlocal means. Pattern Recognition, 47(1): 141-157.

Touzi, R., 2002. A review of speckle filtering in the context of estimation theory. IEEE Transactionson Geoscience and Remote Sensing, 40(11): 2392-2404.

Vasile, G., E. Trouvé, J.S. Lee, V. Buzuloiu, 2006. Intensity-driven adaptive-neighborhood technique for polarimetric and interferometric SAR parameters estimation. IEEE Transactions onGeoscience and Remote Sensing, 44(6): 1609-1621.

Yang, X., D. Clausi, 2009. Structure-preserving speckle reduction of SAR images using nonlocal means filters. 16th IEEE International Conference on Image Processing (ICIP), (pp: 2985-2988).

Zhong, H., Y. Li, L.C. Jiao, 2011. SAR image despeckling using bayesian nonlocal means filter with sigma preselection. Geoscience and Remote Sensing Letters, IEEE, 8(4): 809-813.